Cellular stress created by intermediary metabolite imbalances

Sang Jun Lee[a], Andrei Trostel[a], Phuoc Le[a], Rajendran Harinarayanan[b], Peter C. FitzGerald[c], and Sankar Adhya[a,1]

[a]Laboratory of Molecular Biology, National Cancer Institute, [b]Laboratory of Molecular Genetics, National Institute of Child Health and Human Development, and [c]Genome Analysis Unit, National Cancer Institute, National Institutes of Health, Bethesda, MD 20892

Contributed by Sankar Adhya, September 16, 2009 (sent for review July 14, 2009)

Small molecules generally activate or inhibit gene transcription as externally added substrates or as internally accumulated end-products, respectively. Rarely has a connection been made that links an intracellular intermediary metabolite as a signal of gene expression. We report that a perturbation in the critical step of a metabolic pathway—the D-galactose amphibolic pathway—changes the dynamics of the pathways leading to accumulation of the intermediary metabolite UDP-galactose. This accumulation causes cell stress and transduces signals that alter gene expression so as to cope with the stress by restoring balance in the metabolite pool. This underscores the importance of studying the global effects of alterations in the level of intermediary metabolites in causing stress and coping with it by transducing signals to genes to reach a stable state of equilibrium (homeostasis). Such studies are an essential component in the integration of metabolomics, proteomics, and transcriptomics.

galactose metabolism | gene signals | intracellular stress | tiling arrays

A cell is capable of carrying out thousands of chemical reactions to make or break compounds of different kinds (metabolites). To achieve proper balance in its chemical constituents, these reactions are programmed in time. If there is either a lack or an excess of an important metabolite, it could create stress. The cell is expected to take care of such a stress in two ways: (*i*) The first is a quick fix, which occurs at a biochemical level by activation or inhibition of the catalytic activities of enzymes by metabolites so as to restore homeostasis to the chemical milieu of the cell. (*ii*) The second is a long term solution in which the synthesis of enzymes or proteins whose presence or absence causes the chemical imbalance is turned off or on. These control mechanisms occur at different levels, but the primary level of a metabolite signal is perceived at the level of transcription. So far, the literature describes two classes of metabolites that signal gene transcription: (*i*) a substrate of an enzymatic pathway induces the synthesis of the enzymes of that pathway (usually catabolic), or (*ii*) the end-product of a pathway represses the synthesis of the enzymes of the pathway (usually anabolic). However, except for protein-modifying metabolites, e.g., acetyl-CoA (1, 2) or acetyl-phosphate (3), intermediary metabolites signaling even a specific gene transcription have been reported only in very few cases (4–6). We propose that gene regulation mediated by intermediary metabolites may be more widespread than previously perceived, particularly with respect to the regulation of genes encoding enzymes of amphibolic pathways, in which catabolic pathways overlap with or connect to anabolic pathways. Knowledge of the nature and extent of this type of regulation in an organism is needed for a complete understanding of the genetic regulatory network of cells. We explored one such metabolic intermediate, UDP-galactose, which we found not only sends signals to specific genes to rectify the consequences of its imbalance but, to our surprise and unlike the cases mentioned above (4–6), turns up or down a plethora of other genes, many of whose functions cannot be currently related to the metabolite involved. UDP-galactose is an intermediate in the metabolism of D-galactose, a known amphibolic metabolic pathway. Accumulation of this intermediate was known to cause stress, stop cell growth, and cause cell lysis in complex medium (7–9). Using UDP-galactose as an example, we report here (*i*) that an amphibolic operon is controlled both by the substrate of the pathway and an intermediary product, (*ii*) how the intermediary metabolite accumulation causes cellular stress and sends signals to genetic level, and (*iii*) how the latter overcomes the stress to achieve homeostasis.

Results and Discussion

D-galactose-Dependent Growth Arrest of *gal* Mutants. D-galactose is metabolized by the Leloir pathway, which is conserved from *Escherichia coli* to humans (10). As shown in Fig. 1*A*, the intermediates of the pathway, galactose-1-phosphate, UDP-galactose, UDP-glucose, glucose-1-phosphate, and glucose-6-phosphate can be made both by the forward pathway from D-galactose or by the reverse pathway from nongalactose carbon sources. Two key intermediates are UDP-galactose and UDP-glucose, which connect the amphibolic D-galactose pathway to important glycosylation reactions in macromolecular biosynthesis. The presence of D-galactose during growth of cells defective in genes encoding some of the enzymes in the Leloir pathway causes growth arrest in *E. coli* and galactosemia in humans (7, 9, 11). Although this D-galactose-induced stress has been known for a long time (8), its biochemical mechanism remains unknown. Whereas cells defective in mutarotation (aldose-1-epimerase) and phosphorylation (galactokinase) do not show any growth problem in the presence of D-galactose (supporting information (*SI*) Fig. S1), *E. coli* mutants defective in metabolism of galactose phosphates (*galT*$^-$, *galE*$^-$, and *galU*$^-$) show retarded cell growth in the presence of D-galactose by different amounts (Fig. 2*A*). The amount of growth inhibition was dependent upon concentration of D-galactose. Apparently, accumulation of galactose-phosphate intermediates causes stress and retards cell growth, and this growth inhibition is transient at lower D-galactose concentration. Galactose-1-phosphate accumulation in *galT*$^-$ cells retards cell growth to a lesser extent than other *E. coli* mutant cells (Fig. 2*A*). In *Bacillus subtilis*, accumulation of glucose-1-phosphate caused cell lysis (12). Therefore, sugar phosphate accumulation could be more toxic to cells in some other cases.

The severity of growth arrest by D-galactose addition also depended on the nature of the other carbon source in the growth medium, which was D-fructose in the experiments in Fig. 2*A*. The D-galactose effect was the most severe with the *galE*$^-$ mutant under these growth conditions. In complex medium, severe cell lysis was observed in *galE*$^-$ cells (9); however, only a very small amount of a cell lysis was observed in *galE*$^-$ cells in

Author contributions: S.J.L. and S.A. designed research; S.J.L., A.T., P.L., R.H., and P.C.F. performed research; S.J.L. and S.A. analyzed data; and S.J.L. and S.A. wrote the paper.

The authors declare no conflict of interest.

[1]To whom correspondence should be addressed. E-mail: sadhya@helix.nih.gov.

This article contains supporting information online at www.pnas.org/cgi/content/full/0910586106/DCSupplemental.

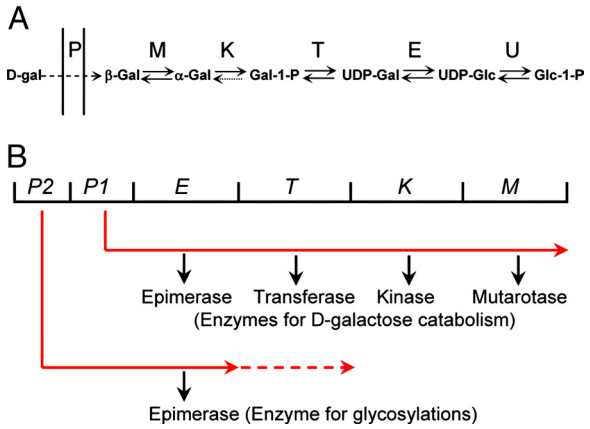

Fig. 1. (*A*) D-galactose metabolism. P, M, K, T, E, and U indicate permeases (GalP and MgI), mutarotase (GalM), galactokinase (GalK), galactose-1-phosphate uridylyltransferase (GalT), UDP-galactose epimerase (GalE), and UDP-glucose pyrophosphorylase (GalU), respectively. (*B*) The structure of *gal* operon. Red lines indicate RNA transcripts from *gal P1* and *P2* promoters.

minimal medium. We further investigated the cause and effect of the growth-arrest phenotype of the *galE*$^-$ mutant.

Difference in D-galactose Metabolism in Wild-Type and *galE*$^-$ Mutant Cells. The net carbon reactions of metabolism of D-galactose in wild type and *galE*$^-$ mutants are compared in Fig. 3*A*. In wild type, one molecule of D-galactose is converted to six molecules of CO_2 and one molecule of ATP, whereas in the *galE*$^-$ mutant, one molecule of D-galactose plus one molecule of UTP are converted to one molecule of UDP-galactose and one molecule of ADP. Because ADP is readily converted back to ATP in the cell, the net result of D-galactose addition to a *galE*$^-$ mutant is expected to be accumulation of UDP-galactose and depletion of UTP. The accumulation of UDP-galactose by D-galactose addition in *galE*$^-$ mutants has been shown previously (9). To confirm that UTP levels decline in these conditions, we analyzed the intracellular UTP levels in wild-type and mutant cells in the presence and absence of D-galactose.

Nucleotide Pool Analysis. Nucleotide pools in cells were analyzed by TLC of total cell extracts. In minimal D-fructose medium, the purine nucleoside triphosphates pool of wild-type *E. coli* was higher than that of pyrimidine nucleoside triphosphates as reported previously (13) and were unaffected by the addition of D-galactose (Fig. 3*B*). However, the UTP pool, as expected, dramatically went down within 5 min after external D-galactose addition in *galE*$^-$ mutant cells. CTP levels subsequently decreased after D-galactose addition, presumably because CTP is made from UTP by CTP synthetase (14). On the other hand, there was a marginal increase, if any, in the concentration of the purine nucleoside triphosphates in *galE*$^-$ mutants in the presence of D-galactose. Addition of nonmetabolizable inducer, D-fucose (6-deoxy-D-galactose), did not change nucleotide pools showing that metabolism of D-galactose is required for UTP depletion (Fig. S2), and UDP-galactose accumulation indeed reduces UTP and as a consequence CTP levels.

Unexpectedly, the level of the alarmone guanosine tetraphosphate (ppGpp), which is chromatographed in the same TLC plates used for nucleoside triphosphates separation and whose level usually increases under cellular stress (15), went down right after D-galactose addition in *galE*$^-$ mutants despite cellular stress. Although the mechanism by which ppGpp levels went down under stressed conditions remains to be investigated, the lowering of ppGpp concentration was consistent with the observation that rRNA synthesis went up after D-galactose addition to *galE*$^-$ cells (see below). Vogel et al. reported that partial pyrimidine auxotrophy leads to an unusually reduced ppGpp pool (16). We thus assume that the decreased ppGpp level is more directly related to UTP deficiency rather than UDP-galactose accumulation.

Consequences of UTP Deficiency in the Cell. Is the growth arrest of *galE*$^-$ mutants by D-galactose a consequence of deficiency of UTP, a building block of RNA? We monitored RNA, DNA, and protein synthesis following D-galactose addition to *galE*$^-$ mutant cells by labeling with [^{3}H]adenosine, [^{3}H]thymidine, and L-[^{35}S]methionine, respectively. The synthesis of total RNA, DNA, and protein were not affected by D-galactose in the wild-type strain (Fig. 2*B*). On the other hand, in *galE*$^-$ mutant cells, the rate of RNA synthesis immediately decreased 5.7-fold after D-galactose addition. DNA replication and protein synthesis gradually decreased thereafter. These results indicate that the D-galactose-induced *galE*$^-$ growth arrest is due to reduced RNA synthesis as a result of low availability of UTP and CTP in the cell.

Transcriptome Analysis by DNA Tiling Arrays. To analyze whether any metabolic imbalance created by accumulation of UDP-galactose or depletion of UTP signals changes in gene expression, we analyzed the transcriptome in wild-type and *galE*$^-$ mutant cells by DNA tiling arrays. DNA tiling array hybridization results, scanned by Affymetrix Gene-chip Scanner 3000, were visualized by an integrated genome browser. In the wild-type cells, the *gal* regulon genes, including the *gal* operon, were clearly derepressed by D-galactose (see model-based analysis of tiling-array (MAT) plot of RNA level in the presence vs. absence of D-galactose in Fig. 2*C*). In addition to the *gal* operon, *galP* (galactose permease), and *mglBAC* (ATP-dependent methyl-galactoside transporter) genes were highly induced by D-galactose in the wild type as expected. Most of the other *E. coli* genes were not affected in wild type by D-galactose addition. The expression of only two nongalactose markers were changed by D-galactose in wild type: *his* (histidine biosynthesis) and *fru* (fructose catabolism) operons. The latter operon, which encodes D-fructose PTS transporter and 1-phosphofructokinase, was downregulated most likely because of a shift in carbon source from D-fructose to D-galactose. We are currently investigating the unexpected derepression of the *his* operon by D-galactose. Surprisingly, the *galE*$^-$ mutant cells grown in the presence of D-galactose showed numerous severely dispersed outliers in the DNA tiling array MAT plot (Fig. 2*C*). We selected genes with twice the standard deviation of distances from a linear fit line in a MAT plot. By the MAT score criteria, 135 genes were upregulated, and 106 genes were downregulated in the *galE*$^-$ mutant by D-galactose addition. Prominent among them are upregulation of rRNA operons, stress responsive genes, and several miscellaneous metabolic genes. Among the downregulated genes were some ribosomal protein genes, several metabolic genes, and two stress responsive proteins. Table S1 provides the complete list of genes whose expressions changed in *galE*$^-$ mutant cells by three times the standard deviation. Thus, D-galactose-induced stress in *galE*$^-$ mutants is associated with changes in gene regulation directly or indirectly. How does the accumulation of UDP-galactose or depletion of UTP send signal to alter the cellular transcription profile? We investigated the mechanism of upregulation of two promoters chosen from among the outliers in the MAT score plot (Fig. 2*C*).

Pathway of Internal Signals to Change Gene Expression. (*i*) Induction of the *P2* promoter of the *gal* operon. The *gal* operon of *E. coli* is transcribed from two promoters, *P1* and *P2* (Fig. 1*B*). *P1* is enhanced and *P2* is inhibited by cAMP·CRP; both are induced by D-galactose, although *P1* is induced more than *P2*. (17).

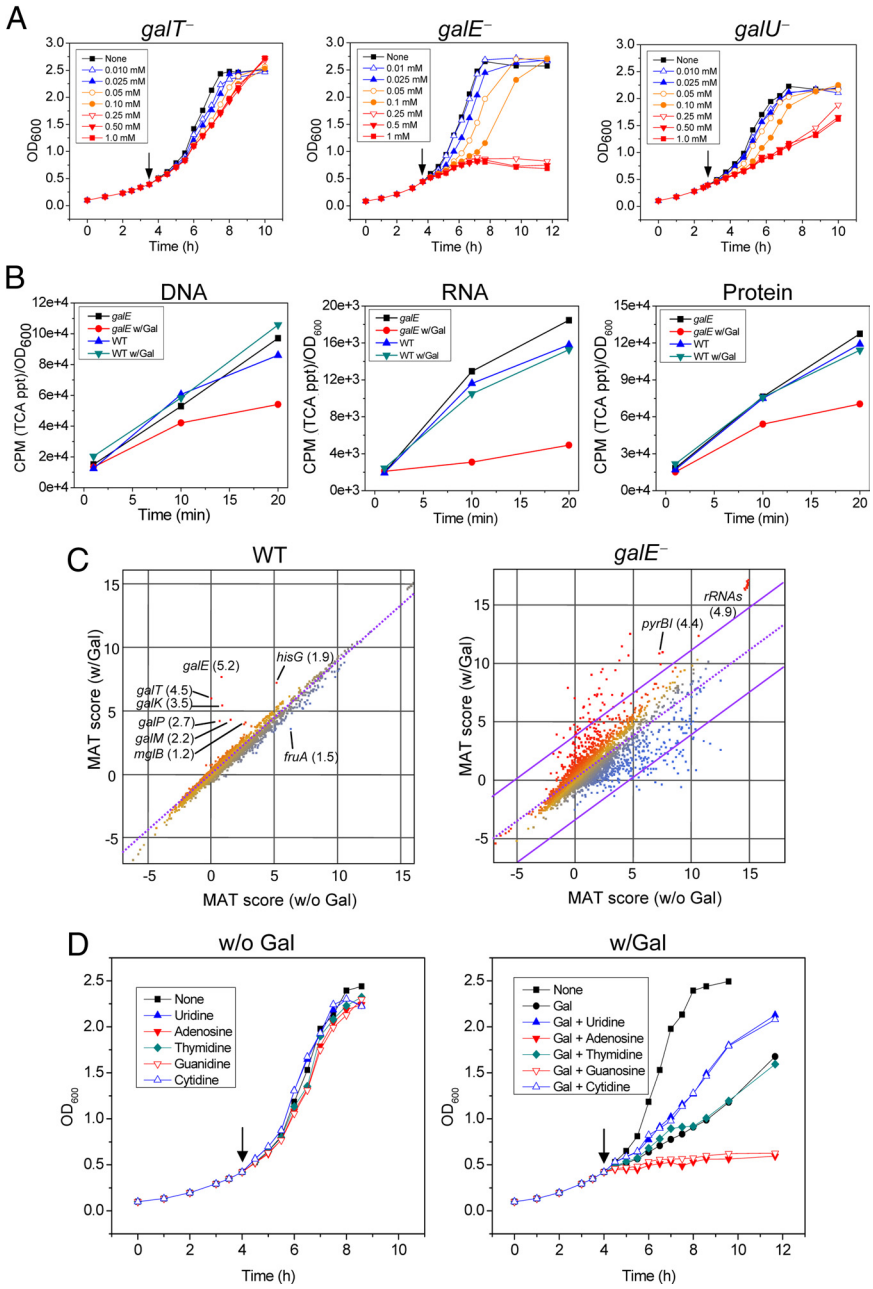

Fig. 2. (*A*) D-galactose concentration-dependent growth arrests in *gal* mutants. Arrows indicate the time of addition of D-galactose. (*B*) In vivo labeling experiment of DNA with thymidine[^{3}H], RNA with adenosine[^{3}H], and protein with methionine[^{35}S] in wild type and *galE*$^-$ mutants in the presence and absence of D-galactose. (*C*) MAT analysis of transcriptomes of wild-type and *galE*$^-$ strains in the presence and absence of D-galactose. In wild type, *gal* regulon members are clearly induced by D-galactose. Among *his* and *fru* operon expressions that were also affected by D-galactose, only *hisG* and *fruA* are marked in MAT plot. In *galE*$^-$, outliers are numerous in response to D-galactose. Dotted purple is a linear fit line. Straight purple indicates three times standard deviation of distances. Numbers in parentheses are distances between coordinates, corresponding genes, and linear fit lines. (*D*) Recovery of D-galactose-induced *galE*$^-$ growth arrests by pyrimidine nucleosides. Nucleosides (0.1 mM) were supplied in the absence and presence of D-galactose (0.1 mM, Gal), respectively. D-galactose concentration used shows transient inhibition of cell growth. Arrows indicate when both D-galactose (0.1 mM), and nucleosides (0.1 mM) were added.

Under conditions of cAMP·CRP deficiency, *P2* becomes the more active promoter. It has been shown that the *P2* promoter primarily makes the *galE* gene product, UDP-galactose epimerase, which metabolizes UDP-galactose (18, 19). The *gal* operon is partially induced even in the absence of D-galactose. The sensitivity of the tiling arrays does not allow a distinction between *P1*- and *P2*-mediated *gal* transcription. Does accumulation of UDP-galactose or any other intermediate cause induction of *gal* transcription in the *galE*$^-$ mutant cells? In vitro transcription assays showed that only D-galactose and not any of the metabolic intermediates, galactose-1-phosphate, UDP-galactose, or UDP-glucose, acts as an inducer of *P1* or *P2* transcription (20). Thus the accumulated UDP-galactose is unlikely to modulate *gal* transcription directly in vivo. The follow-up question remained whether UTP depletion causes induction of *gal* in the *galE*$^-$ cells. Interestingly, it was previously shown that the *P2*, not the *P1*, promoter of *gal* is under UTP-mediated stuttering control (21). The second, third, and fourth positions of *P2* RNA are uridine residues (Fig. 4*A*). Under conditions of UTP limitation, productive mRNAs were made

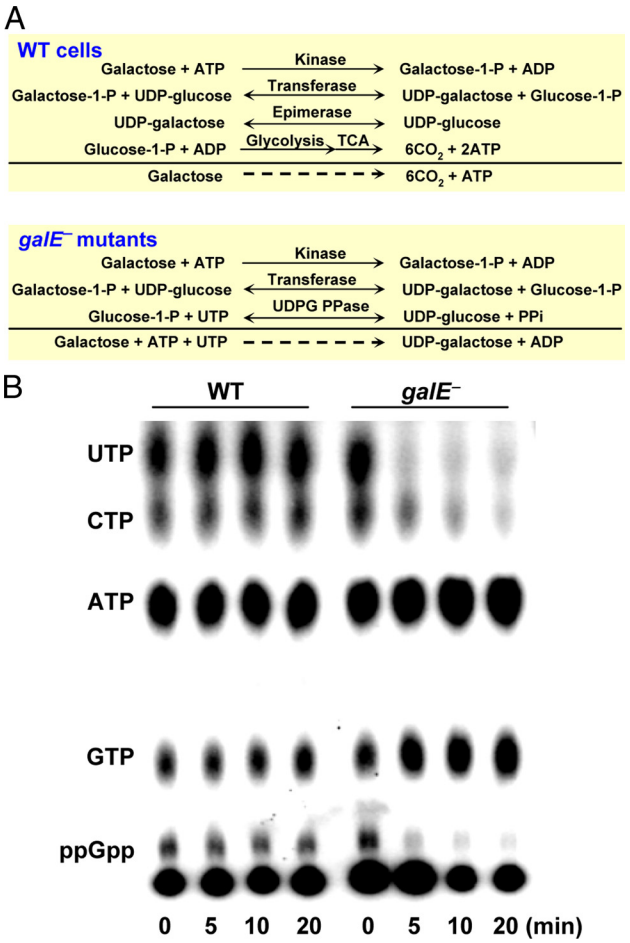

Fig. 3. (*A*) Net difference in D-galactose metabolism in between wild type and *galE*$^-$ mutant. (*B*) TLC of ^{32}P-labeled nucleotides of wild type and *galE*$^-$ mutants in the presence of D-galactose. Numbers indicate time (min) after D-galactose addition in the cells.

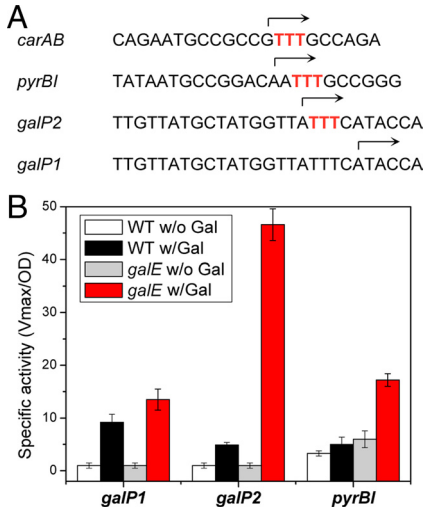

Fig. 4. (*A*) Repetitive thymidine residues (red) at the transcription initiation regions, which cause UTP-dependent stuttering transcription discussed in text. *galP1* sequence shown for comparison. (*B*) In vivo reporter gene assay of *galP1*, *galP2*, and *pyrBI* promoters in the presence and absence of D-galactose in wild-type and *galE*$^-$ mutant strains.

both from *P1* and *P2* promoters in vitro. However, when the UTP levels are high, RNA polymerase at the *P2*, not *P1*, promoter stutters at the 2–4 positions making $A(U)_n$ products, with n being 3 and more, and not productive mRNA (21). If the presence of D-galactose makes *galE*$^-$ mutant UTP deficient, as shown above, then we hypothesize that the *P2* promoter in *gal* would be further derepressed by eliminating stuttering. We fused a reporter gene, *gus*, encoding β-glucuronidase, individually to the *P1* and *P2* promoter at the *gus* locus in the *E. coli* chromosome (20). The fusions of *P1* and *P2* were introduced into wild-type *gal*$^+$ and *galE*$^-$ mutant cells and β-glucuronidase activities were measured in the presence and absence of D-galactose. The results clearly show that, as compared to the *P1* promoter, the *P2* promoter is induced to a much higher level by D-galactose addition in the *galE*$^-$ mutant cells than in wild type (Fig. 4*B*). First, this indicates that the DNA tiling array data of increased *gal* transcription represents *P2* induction. Second, it strongly supports our hypothesis that UDP-galactose accumulation-mediated UTP depletion increases *P2* promoter activity through its UTP-mediated stuttering regulation. (*ii*) Derepression of pyrimidine biosynthetic genes by UDP-galactose. If it is true that *P2* upregulation in *gal* is because of the suppression of stuttering caused by UTP depletion, then one would expect that expression of other promoters with UTP-stuttering control would also be derepressed by D-galactose in the *galE*$^-$ mutant. This was indeed hinted at in the tiling array results, which showed derepression of the *E. coli* pyrimidine biosynthetic operons including P_{pyrBI} and P_{carAB} (Fig. 2*C*; Table S2). In these two operons, three uridine residues start at position +2. Excess UTP levels cause stuttering at the uridine clusters, and UTP limitation derepresses these operons both in vivo and in vitro (*22*). Assay of β-galactosidase levels in a P_{pyrBI}-*lacZ* fusion in the *galE*$^-$ mutant, showed that addition of D-galactose raised the P_{pyrBI} expression about 2.9-fold (Fig. 4*B*).

Together, derepression of *P2* and P_{pyrBI} by addition of D-galactose in the *galE*$^-$ mutant demonstrate that accumulation of a metabolic intermediate, UDP-galactose, and consequent depletion of UTP by a perturbation of the pathway (by a mutation in our experiments), signal gene expressions to restore the two metabolites to their original levels by making more GalE enzyme to use up UDP-galactose and by derepressing the pyrimidine biosynthetic enzymes to increase UTP and CTP levels, respectively.

Reversal of D-galactose-Induced Growth Arrest by Pyrimidine Supplements. To confirm that the pyrimidine deficiency is the primary reason for the growth arrest of *galE*$^-$ cells by D-galactose, we added different bases or nucleosides in the cell culture for relief from D-galactose-induced stress (Fig. 2*D*). Whereas addition of 0.1 mM uridine, cytidine, thymidine, adenosine, or guanosine did not affect *galE*$^-$ cell growth in the absence of D-galactose, uridine and/or cytidine did help to relieve the inhibition of cell growth caused by D-galactose. Addition of higher concentrations of uridine or cytidine restored growth almost fully. More or less identical results were obtained with the corresponding bases (Fig. S3). Thymidine addition did not have any influence on cell growth under similar conditions. Note that cytidine and uridine are interconvertible in vivo but thymidine (a deoxy nucleoside) is not. Interestingly, addition of purine nucleosides (guanidine and adenosine) makes D-galactose more toxic to cells, presumably because purine nucleoside addition makes the ratio of pyrimidines to purines in the nucleosidetriphosphates pool detrimentally unbalanced in the cell. When a pyrimidine base or nucleoside was added to the mutant cultures even 1 h after D-galactose addition, it helped to restore the cell growth (Fig. S4). These results demonstrate that bacteriostasis of *galE*$^-$ mutants in the presence of D-galactose directly comes from pyrimidine deficiency or an unbalanced

nucleotide pool. In complex media, severe lysis was observed in *galE*$^-$ mutant cells. This might be because enough uridine and cytidine are imported from the media to support RNA synthesis, yet do not suffice for making enough UDP intermediates such as UDP-glucose for peptidoglycan synthesis.

In summary, although shown above for UDP-galactose, we propose that at crossroads of metabolic pathways there are intermediary metabolites whose imbalances cause stress that send signals to genes to rectify the stress and achieve homeostasis. Given current technology of metabolomics (23), it is now feasible to integrate metabolomics to gene expressions. Metabolic disorders because of inherited mutations in animals and human, originally called "molecular diseases" are very likely because of alteration of normal flux of metabolites in cells. The associated phenotypes of such diseases may originate from changes in gene expression pattern. Then one may identify compensatory metabolites to remove the symptoms.

Materials and Methods

Strains and Growth Curves. Individual *gal* mutant strains were from the Keio collection (24). To make isogenic strains, P1 lysates of Keio collections were used to transduce *galT*$^-$, *galE*$^-$, and *galU*$^-$ mutations carrying kanamycin markers into BW25113 wild-type strain. Subsequently, pCP20 (25) were transformed into *galT*$^-$ and *galE*$^-$ mutants to delete kanamycin marker, to avoid an unwanted transcriptional polarity of *gal*. After removing kanamycin marker, the temperature-sensitive pCP20 plasmid was cured at 42 °C.

For D-galactose concentration-dependent growth-arrest experiments, each mutant was grown in three different media, LB, M63 minimal media containing 0.3% D-fructose, or 0.3% D-glycerol in the presence of D-galactose concentrations (0.01 to 1 mM) at 37 °C. Overnight cell cultures were diluted 1:3 or 1:5 in the same media to accurately measure the optical density during subsequent growth. The optical density of cell cultures at 600 nm was monitored for cell growth using Ultrospec 3100 pro spectrophotometer (Amersham Biosciences).

TLC Assay. Nucleotide triphosphate pools were analyzed by TLC as previously described (26). Cells were grown in high phosphate (final 1.3 mM) Mops media overnight and then transferred to low phosphate (final 0.3 mM) Mops media. At OD_{600} = 0.2, inorganic phosphate (^{32}P, final 150 μCi/mL) was added for labeling of nucleotide phosphates. At OD_{600} = 0.4, D-galactose (final 0.3%) or D-fucose (final 0.3%) were added. Ten-microliter samples were taken and mixed with 10 μL of 2 N formic acid and immediately chilled in dry ice. More than three times, freeze and thaw cycle lysed cells. Four microliters of each lysate was equilibrated to pH 7.0 with Tris-base solutions and were loaded on poly(ethylene)imine cellulose TLC plates and chromatographed in phosphate buffer.

Radioactive Labeling of Total DNA, RNA, and Protein. All radioactive chemicals were purchased from MP Biomedicals. [Methyl-^{3}H]thymidine (72.1 Ci/mmol, 1 mCi/mL, cat. no. 012406001), [2, 8-^{3}H]adenosine (25 Ci/mmol, 1 mCi/mL, cat. no. 0124400801), and L-[^{35}S]methionine (1175 Ci/mmol, 10 mCi/mL, cat. no. 51001H) were used for labeling of newly synthesized DNA, RNA, and protein, respectively. Stock solutions for DNA, RNA, and protein labeling were made as follows: 1 mL of thymidine labeling stock solution (20 μCi/mL) was made by mixing 20 μL of radioactive thymidine and 980 μL of 5 mM cold thymidine; 1 mL of L-methionine stock solution (100 μCi/mL) was made by mixing 10 μL of L-[^{35}S]methionine and 990 μL of 5 mM cold L-methionine, and 1 mL of radioactive adenosine stock solution (20 μCi/mL) was made by mixing 20 μL of radioactive adenosine and 980 μL of 5 mM cold adenosine. Labeling protocols of nucleic acids and proteins by radioactive precursors were slightly modified from ref. 27 as follows: At OD_{600} = 0.5, 0.2 mL of labeled thymidine (20 μCi/mL, 5 mM), adenosine (20 μCi/mL, 5 mM), and L-methionine (100 μCi/mL, 5 mM) at final concentration of 50 μM, respectively, were added to 20-mL flasks of cell cultures growing in M63 minimal medium containing D-fructose (final 0.3%) grown at 37 °C. At the same time, D-galactose (final 0.3%) was added when needed. Samples were taken from the cultures at 0 min and subsequently 500 μL samples were taken every 10 min, immediately transferred to Eppendorf tubes that contained 10% TCA cold solutions (500 μL), vortexed, and then chilled on ice. Samples were transferred onto glass microfiber filters (Whatman cat. no. 1822024; 2.4 cm) that were connected to a vacuum apparatus. The filters were washed twice with 5% TCA with ethanol, dried, and put into vials containing 5 mL of Ecoscint A solution (National Diagnostics). Counts per minute were measured using a LS6500 liquid scintillation counter (Beckman Coulter).

DNA Tiling Arrays. Tiling array chips (Ecoli_Tab520346F) were purchased from Affymetrix. The chips had 1,159,908 probes in 1.4 cm × 1.4 cm and a 25-mer probe every 8 bp in both strands of the entire *E. coli* genome. The probes overlapped by 4 bp with the opposite strand probes. Each 25-mer DNA probe in the tiling array chip are 8 bp apart from the next probe and designed to cover the whole *E. coli* genome. Sample processing was performed according to the Affymetrix GeneChip Expression Analysis Technical Manual, Section 3: Prokaryotic Sample and Array Processing (701029 Rev.4). For DNA tiling array experiments, *E. coli* K-12 BW25113 and its isogenic mutants were grown in 125-mL corning flasks containing 30 mL of M63 minimal medium plus D-fructose (final 0.3%) at 37 °C. At OD_{600} 0.5, cell cultures were separated into two flasks. D-galactose (final 0.3%) was added to one and cells were cultivated for 1.5 h further.

cDNA Synthesis, Labeling, and Hybridization. Cells were then placed on ice and RNAprotect bacteria reagent, 76506 (Qiagen) was added to stabilize the RNA. Cells were then harvested for RNA purification by RNeasy mini kit, 74104 (Qiagen). Isolated RNA (10 μg) was used for random primer cDNA synthesis using SuperScript II reverse transcriptase, 18064–071 (Invitrogen). The reaction mixture was then subsequently treated with 1 N NaOH to degrade any remaining RNA and treated with 1 N HCl to neutralize the NaOH. Synthesized cDNA was then purified using MiniElute PCR purification columns, 28004 (Qiagen). Purified cDNA (3 μg) was fragmented to between 50 and 200 bps by 0.6 U/μg of DNase I, 27–0514-01 (Amersham Biosciences) for 10 min at 37 °C in 1× One-Phor-All buffer, 27–0901-02 (Amersham Biosciences). Heat inactivation of the DNase I enzyme was performed at 98 °C for 10 min. Fragmented cDNA was then 3′ termini biotin-labeled using the GeneChip DNA labeling reagent, 900542 (Affymetrix) and 60 U of terminal deoxynucleotidyl transferase, M1875 (Promega) at 37 °C for 1 h. The labeling reaction was then stopped by the addition of 0.5 M EDTA. Labeled cDNA fragments (3 μg) were hybridized at 45 °C at 60 rpm for 16 h to the tiling array chips. The chips were then washed with wash buffer A: nonstringent wash buffer (6X SSPE, 0.01% Tween-20); wash buffer B: (100 mM Mes, 0.1M [Na^+], 0.01% Tween-20) and stained with streptavidin phycoerythrin (Invitrogen, S-866) and anti-streptavidin goat antibody biotinylated (Vector Laboratories, BA-0500) on a Genechip Fluidics Station 450 (Affymetrix) according to washing and staining protocol (ProkGE-WS2_450).

Tiling Array Data Analysis. Hybridized, washed, and stained tiling arrays were scanned using a Genechip Scanner 3000 (Affymetrix). Standardized signals, for each probe in the arrays, were generated using the MAT software (28), which provides a model-based, sequence-specific, background correction for each sample. A gene-specific score was then calculated for each gene by averaging all MAT scores (natural log) for all probes under the annotated gene coordinates. Gene annotation was from the ASAP database (29) at the University of Wisconsin-Madison, for *E. coli* K-12 MG1655 version m56. Differences of two log scale values in the absence or presence of D-galactose were calculated in the mutants. Then, the genes showing more than three times standard deviation from the mean signal difference were selected and listed in Table S1. ArrayStar software (DNASTAR) was used for diagonal visualization of the data.

Reporter Gene Assay. *E. coli* CLT5307 strain was kindly supplied by C. L. Turnbough, Jr. (University of Alabama, Birmingham). Lysogenic phage carrying *pyrBI-lacZ* and ampicillin resistance in CLT5307 was transferred to wild-type and *galE*$^-$ strains. After the cells were grown to OD_{600} of 0.5 in M63 minimal medium containing 0.3% D-fructose and 0.1% casamino acids, 0.3% D-galactose was added and cells were further grown for 1.5 h. The activity of β-galactosidase synthesis in cells was measured as described previously (30). Gus assay of *galP1* and *-P2* was carried out as previously described (20).

Nucleoside Supplementation Assay. All nucleosides were purchased from Sigma-Aldrich and dissolved in DMSO to make stock solutions (final 250 mM). Nucleosides (final 0.1 mM) and/or D-galactose (final 0.1 mM) were added at OD_{600} = 0.4 during cell growth in M63 minimal medium (20 mL in 125-mL flask) containing 0.3% D-fructose. The optical density of cell cultures at 600 nm was monitored for cell growth using an Ultrospec 3100 pro spectrophotometer (Amersham Biosciences).

ACKNOWLEDGMENTS. We thank R. Edgar, D. E. A. Lewis, M. Cashel for helpful discussions, and R. Edgar and R. A. Weisberg for critical reading of the manuscript and suggestions. We thank D. J. Jin and C. L. Turnbough, Jr. for the gift of bacterial strains. This work was supported by the Intramural Research Program of the National Institutes of Health, National Cancer Institute, Center for Cancer Research.

1. Yang XJ, Seto E (2008) Lysine acetylation: Codified crosstalk with other posttranslational modifications. *Mol Cell* 31:449–461.
2. Zhang J, et al. (2009) Lysine acetylation is a highly abundant and evolutionarily conserved modification in *Escherichia coli*. *Mol Cell Proteomics* 8:215–225.
3. Klein AH, Shulla A, Reimann SA, Keating DH, Wolfe AJ (2007) The intracellular concentration of acetyl phosphate in *Escherichia coli* is sufficient for direct phosphorylation of two-component response regulators. *J Bacteriol* 189:5574–5581.
4. Bohringer J, Fischer D, Mosler G, Hengge-Aronis R (1995) UDP-glucose is a potential intracellular signal molecule in the control of expression of sigma S and sigma S-dependent genes in *Escherichia coli*. *J Bacteriol* 177:413–422.
5. Persson O, Valadi A, Nystrom T, Farewell A (2007) Metabolic control of the *Escherichia coli* universal stress protein response through fructose-6-phosphate. *Mol Microbiol* 65:968–978.
6. Tweeddale H, Notley-McRobb L, Ferenci T (1998) Effect of slow growth on metabolism of *Escherichia coli*, as revealed by global metabolite pool (''metabolome'') analysis. *J Bacteriol* 180:5109–5116.
7. Kalckar HM (1960) Hereditary defects in galactose metabolism in man and microorganisms. *Fed Proc* 19:984–990.
8. Kalckar HM, Kurahashi K, Jordan E (1959) Hereditary defects in galactose metabolism in *Escherichia coli* mutants, I. Determination of Enzyme Activities. *Proc Natl Acad Sci USA* 45:1776–1786.
9. Nikaido H (1961) Galactose-sensitive mutants of *Salmonella*. I. Metabolism of galactose. *Biochim Biophys Acta* 48:460–469.
10. Fridovich-Keil JL (2006) Galactosemia: The good, the bad, and the unknown. *J Cell Physiol* 209:701–705.
11. Sundararajan TA (1963) Interference with glycerokinase induction in mutants of *E. coli* accumulating Gal-1-P. *Proc Natl Acad Sci USA* 50:463–469.
12. Prasad C, Freese E (1974) Cell lysis of *Bacillus subtilis* caused by intracellular accumulation of glucose-1-phosphate. *J Bacteriol* 118:1111–1122.
13. Buckstein MH, He J, Rubin H (2008) Characterization of nucleotide pools as a function of physiological state in *Escherichia coli*. *J Bacteriol* 190:718–726.
14. Long CW, Pardee AB (1967) Cytidine triphosphate synthetase of *Escherichia coli* B. I. Purification and kinetics. *J Biol Chem* 242:4715–4721.
15. Potrykus K, Cashel M (2008) (p) ppGpp: Still magical? *Annu Rev Microbiol* 62:35–51.
16. Vogel U, Pedersen S, Jensen KF (1991) An unusual correlation between ppGpp pool size and rate of ribosome synthesis during partial pyrimidine starvation of *Escherichia coli*. *J Bacteriol* 173:1168–1174.
17. Adhya S, Miller W (1979) Modulation of the two promoters of the galactose operon of *Escherichia coli*. *Nature* 279:492–494.
18. Adhya S (1987) The galactose operon *Escherichia coli* and *Salmonella*: Cellular and molecular biology (American Society for Microbiology, Washington, DC) pp 1503–1512.
19. Lee HJ, Jeon HJ, Ji SC, Yun SH, Lim HM (2008) Establishment of an mRNA gradient depends on the promoter: An investigation of polarity in gene expression. *J Mol Biol* 378:318–327.
20. Lee SJ, Lewis DE, Adhya S (2008) Induction of the galactose enzymes in *Escherichia coli* is independent of the C-1-hydroxyl optical configuration of the inducer D-galactose. *J Bacteriol* 190:7932–7938.
21. Jin DJ (1994) Slippage synthesis at the *galP2* promoter of *Escherichia coli* and its regulation by UTP concentration and cAMP.cAMP receptor protein. *J Biol Chem* 269:17221–17227.
22. Turnbough CL, Jr, Switzer RL (2008) Regulation of pyrimidine biosynthetic gene expression in bacteria: Repression without repressors. *Microbiol Mol Biol Rev* 72:266–300.
23. Weckwerth W (2003) Metabolomics in systems biology. *Annu Rev Plant Biol* 54:669.
24. Baba T, et al. (2006) Construction of *Escherichia coli* K-12 in-frame, single-gene knockout mutants: The Keio collection. *Mol Syst Biol* 2:2006.0008.
25. Cherepanov PP, Wackernagel W (1995) Gene disruption in *Escherichia coli*: TcR and KmR cassettes with the option of Flp-catalyzed excision of the antibiotic-resistance determinant. *Gene* 158:9–14.
26. Cashel M, Lazzarini RA, Kalbacher B (1969) An improved method for thin-layer chromatography of nucleotide mixtures containing 32P-labelled orthophosphate. *J Chromatogr* 40:103–109.
27. Glaser VM, al-Nuri MA, Groshev VV, Shestakov SV (1973) The labeling of nucleic acids by radioactive precursors in the blue-green algae *Anacystis nidulans* and Synechocystis aquatilis Sanv. *Arch Mikrobiol* 92:217–226.
28. Johnson WE, et al. (2006) Model-based analysis of tiling-arrays for ChIP-chip. *Proc Natl Acad Sci USA* 103:12457–12462.
29. Glasner JD, et al. (2003) ASAP, a systematic annotation package for community analysis of genomes. *Nucleic Acids Res* 31:147–151.
30. Lewis DE, Geanacopoulos M, Adhya S (1999) Role of HU and DNA supercoiling in transcription repression: Specialized nucleoprotein repression complex at gal promoters in *Escherichia coli*. *Mol Microbiol* 31:451–461.